BNL--45443

DE91 009439

HIGH CURRENT PHOTOEMISSION WITH 10 PICOSECOND UV PULSES*

J. Fischer, T. Srinivasan-Rao, and T. Tsang

Brookhaven National Laboratory, Upton, NY 11973

June 1990

***This research was supported by the U. S. Department of Energy: Contract No. DE-AC02-76CH00016.**

DISCLAIMER

HIGH CURRENT PHOTOEMISSION WITH 10 PICOSECOND UV PULSES*

J. Fischer, T. Srinivasan-Rao, and T. Tsang
Brookhaven National Laboratory, Upton, NY 11973

ABSTRACT

The quantum efficiency and the optical damage threshold of various metals were explored with 10 ps, 266 nm, UV laser pulses. Efficiencies for Cu, Y, and Sm were: 1.4, 5, and 7×10^{-4}, with damage thresholds about 100, 10, and 30 mJ/cm^2. This would permit over 1 μC/cm^2 or current densities exceeding 100 kA/cm^2. High charge and current densities of up to 66 kA/cm^2 were obtained on 0.25 mm diam cathodes, and 21 kA/cm^2 on a 3 mm diam yttrium cathode. The maximum currents were limited by space charge and the dc field. The experiments with small area illumination indicate that the emitted electrons spread transversely due to Coulomb repulsion and their initial transverse velocity. This increases the effective area above the cathode, reduces the space charge effect and increases emission density on the cathode. The quantum efficiency can be increased substantially by enhancing the field on the surface by either a suitable electrode geometry or microstructures on it.

---

*This research was supported by the U.S. Department of Energy: Contract No. DE-AC02-76CH00016.

INTRODUCTION

Short pulse photoemission from photocathodes can be conveniently produced by picosecond lasers which can also control of the intensity, spatial distribution and duration of the electron emission.

Common metal cathodes can provide high current densities because of their large number of free electrons, but they have a low quantum efficiency even with UV beams. However, the common metals are rugged, not very reactive, can operate at moderate vacuum, can withstand high fields and have a long life. These properties make them attractive for applications requiring short duration high current emission such as the switch power Linac (SPL),[1] high brightness electron beam sources for high energy particle colliders, free electron lasers, microwave sources, etc.

The required cathode performances for these applications can be difficult to achieve. As an example these photocathodes for SPL have to: a) be rugged and tolerant to relatively poor vacuum $\sim 10^{-7}-10^{-8}$ Torr, b) require minimum processing, c) emit electrons promptly with <1 ps temporal spread over the irradiating laser pulse, d) be capable of yielding peak current densities exceeding 100 kA/cm^2 in a pulse length <10 ps, e) have UV incident photon to electron conversion (quantum) efficiency $>10^{-3}$, f) be capable of holding off high fields (a few 10^8 V/m) for a few nanoseconds without suffering electrical breakdown, and g) have a long life time with easy rejuvenation.

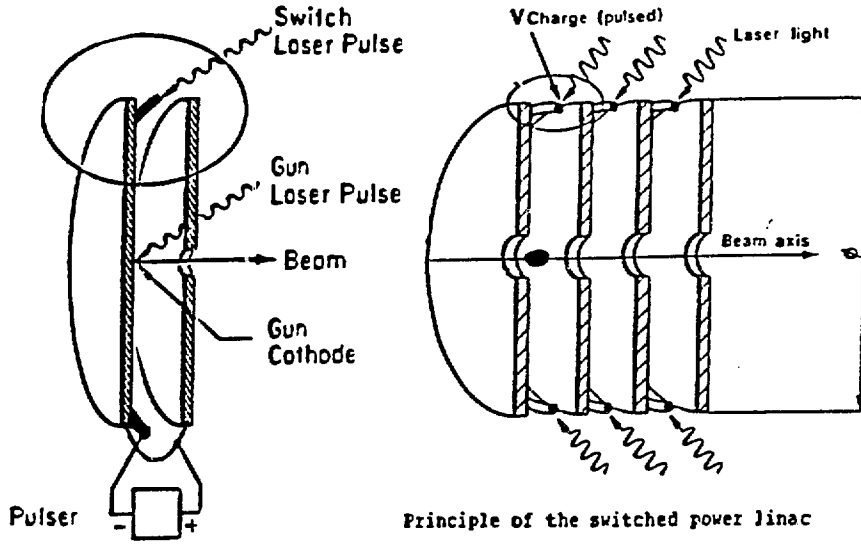

Fig. 1. Accelerating structure for Switch Power Linac showing the ring-shaped photocathode. The first section is an e-gun with a small photocathode at its center.

We studied photoemission from metal photocathodes under non-ideal conditions to be expected in such applications. The cathodes were commercial metals of high purity. After installation in the photodiode cell in a vacuum of $\sim 10^{-8}$ Torr, they were activated with an intense UV beam, 266 nm, 10 ps, 10 Hz, from a quadrupled Nd:YAG laser, which was also used for the emission experiments. A dc field was used for simplicity. In the future higher pulsed fields will be tried. Most of the derived quantities are based on the measured charge emitted by the cathode for each laser pulse of known energy. The efficiencies, current and current densities as calculated, are those experienced at the cathode surface, for the illuminated area, during the laser pulse duration. The emission from metals can be considered here as prompt. However, space charge, the electric field and cathode to anode gap length can increase the electron bunch length arriving at the anode.[2)]

The rest of the papers is arranged in the following order:

1. Experimental Arrangement
2. Quantum Efficiencies, Optical Damage Thresholds and Maximum Current Densities
3. High Current Density Measurements
4. Charge Spreading and Maximum Emitted Charge
5. Improvements of the Quantum Efficiency
   a. Field Assisted Photoemission
   b. Efficiency Increase by Structured Surfaces and Field Assistance
6. High Voltage Breakdown Considerations
7. Conclusions

Some of the experimental measurements, results and discussions are described in detail elsewhere.[3,4)]

1. EXPERIMENTAL ARRANGEMENT

A. Laser and Photodiode

The laser used in these experiments is a 10 Hz Nd:YAG laser (Quantel YG 501 DP) which yields amplified infrared pulses of 1.06 μm wavelength, 25 ps duration, and ~25 mJ energy. This radiation is frequency quadrupled to yield 1.5 mJ of UV radiation at 266 nm with a pulse duration of ~10 ps. This UV beam is passed through a series of mirrors, irises, attenuators and lenses so that the spot size, spatial profile, and energy of the beam can be controlled and monitored before it irradiates the cathode. The schematic of the experimental arrangement is shown in Fig. 2.

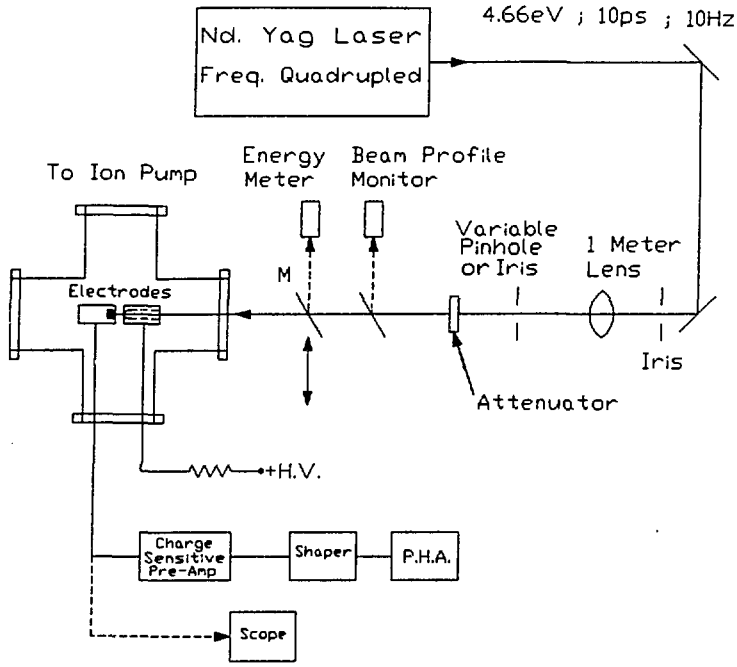

Fig. 2. Schematic of the experimental arrangement.

The vacuum cell, which houses the photodiode, consists of a stainless steel six-way cross. The UV laser beam enters via a sapphire window. The pressure in the cell can be maintained at $10^{-8}-10^{-9}$ Torr with turbo and ion pumps. The electrodes are arranged in the middle of the cell so that the cathode will be illuminated by the laser beam at normal incidence. DC voltages up to 10 kV can be applied to the anode via a resistance of 10−100 MΩ. The information about the charge emitted from the cathode is fed into either a calibrated charge preamplifier, shaping amplifier and pulse height analyzer, or coupled directly from the cell to a fast oscilloscope (Tektronix 7104 or a noncommercial 60 ps rise time oscilloscope on loan from Los Alamos National Laboratory).

The photodiode consists of a flat metal cathode held parallel to a flat anode (Fig. 3). The cathode is illuminated at normal incidence by the laser light passing through a 3–5 mm diameter hole in the anode covered by a fine wire mesh. The electrode gap is variable from 0.3–3 mm. The gaps and the mesh sizes are chosen so that the field lines at the emitting area would not be distorted strongly by the wire mesh. With this electrode geometry, the emitting area and its shape or aspect ratio could be varied over a wide range so that the scaling of the electron emission with area at high current densities could be studied.

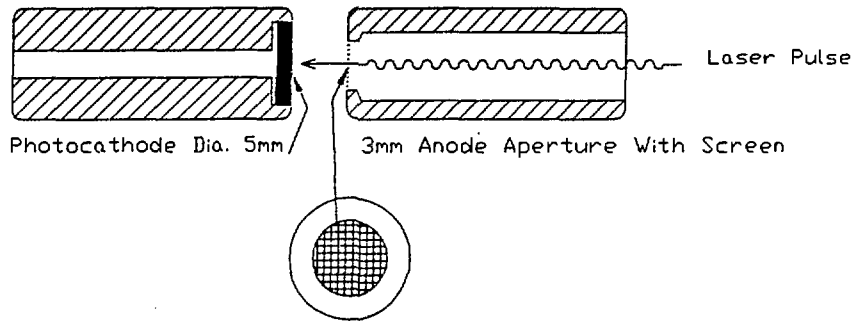

Fig. 3. Electrode Configuration: The flat cathode is held parallel to the anode. The laser beam passes through a fine conductive mesh that covers the hole in the anode. The electrode gap can be varied from 0.3 to 3 mm.

B. Photocathode Preparation

The surface quality and purity of the cathode can critically determine the efficiency of the photoelectric conversion. Our results have to be considered in relation to this particular preparation.

The flat photocathodes are made of small high purity sheet metal discs, machined from the desired metal. The discs are soldered to the end of cylindrical copper electrodes, and then lapped with a 1 μm diamond compound, washed in solvents, ultrasonically cleaned and stored in hexane topped with N_2. When setting the electrode gap, the photocathode experiences a brief 1−2 minute exposure to air. The assembly is then cleaned under a N_2 jet and installed in the test cell, which is filled with N_2. The cell is then evacuated, baked at ~150°C, and pumped to a pressure of $\sim 10^{-8}-10^{-9}$ Torr at room temperature.

To activate the photocathode, the surface is irradiated with the 266 nm (4.66 eV) laser beam with an energy density of 3−5 mJ/cm^2 for 5−10 minutes before the measurements. During the activation process, the pressure increases temporarily; the quantum efficiencies increases, in some cases, up to four order of magnitude. After the activation, the efficiency decreases slowly in time. The decay rate depends on the quality of the vacuum, and the type of metal, e.g., gold decayed least. The efficiency could be restored by reactivation with UV beam.

2. QUANTUM EFFICIENCIES, DAMAGE THRESHOLDS AND MAXIMUM CURRENT DENSITIES

A. Quantum Efficiencies

These are defined as the number of electrons per incident photon of 4.66 eV in this case. These were measured at low intensities under emission limited conditions. The results are listed in Table 1 along with their published work functions.[5)]

Table 1. Work Functions and Observed Quantum Efficiencies[a)] (No Space Charge)

Material	Work Function (eV)	Efficiency Measured at Low Fields (10^{-3})
Palladium	5.	.012
Nickel	4.4	.025
Zirconium	4.3	.01
Gold	4.3	.047
Copper	4.3	.14
Silver	4.3	.02
Tantalum	4.25	.01
Zinc	3.7	.014
Magnesium	3.66	.62
Terbium	3.0	.235
Yttrium	2.9	.5
Samarium	2.7	.725

[a]UV beam: 4.66 eV; 10 ps; 10 Hz

To the first order approximation, for $h\nu > \phi$, the quantum efficiency can be expressed[6)] as

$$\eta = A(h\nu - \phi)^2 \qquad (1)$$

where A is a constant that depends on material properties such as the absorption coefficient, density of states, transition probability, and the angle of incidence of the laser light. ϕ is the work function of the material and $h\nu$ is the photon energy. As can be seen from Table 1, the efficiency increases roughly with the decrease of the work function. But the presence of the surface contaminants and the roughness, along with the lack of complete information about the density of states and the transition probabilities make theoretical evaluation of η very difficult. However, the efficiencies we have measured with gold, a metal less susceptible to contamination, are comparable to that of other experimenters.[7] For the photon energy of 4.66 eV, magnesium, yttrium, and samarium exhibit quantum efficiencies exceeding 5×10^{-4}. The quantum efficiency of copper, 1.4×10^{-4}, is surprisingly high for a material with such high work function.

B. Optical Damage Thresholds and Maximum Current Densities

Damage thresholds were determined for Y, Cu, Au, Sm by microscopic examination of these cathodes exposed to about 3000 laser pulses of 10 ps, 4.66 eV photons at varying intensities.

The maximum current densities at damage threshold can then be calculated from the respective quantum efficiencies for these materials as shown in Table 2.

The results show that assuming sufficient extraction fields, the current densities of over 100 kA/cm^2 needed for the SPL may be achieved for some

metals, without optically damaging the photocathode surface. Higher current densities are possible for shorter laser pulses, since at these pulse durations, the optical damage threshold (expressed as energy per unit area) is independent of the pulse duration[8] but current density is inversely proportional to the electron (laser) pulse duration.

Table 2

	Y	Cu	Au	Sm
Damage Threshold (mJ/cm^2)	~10	~100	~100	~30
Quantum Efficiency	$\sim 5\times10^{-4}$	$\sim 1.4\times10^{-4}$	$\sim 5\times10^{-5}$	$\sim 5\times10^{-4}$
Maximum Charge ($\mu C/cm^2$)	~1	~3	~1	~4
J_{max} (kA/cm^2)	~100	~300	~100	~400

In any case, an improvement of the quantum efficiency (see Section 6), will increase the safe maximum current density.

3. HIGH CHARGE AND CURRENT DENSITY MEASUREMENTS

In practical applications the maximum achievable current density is limited not only by the optical damage threshold, but also by the extraction field, and by space charge effects which reduce the effective field on the cathode surface and thereby reduce the emission currents. Space charge can also increase the electron bunch length as it drifts to the anode.[2] The stored charge in the diode system and the diode and photon beam geometry can also impose additional limitations on the maximum charge that can be

extracted. (For our cases we assume that the emission duration at the cathode is the same as that of the laser pulse.)

Figures 4a and 4b illustrate the emitted charge vs. field for Sm and Mg for a laser energy of 1.10 and 3.12 μJ, respectively. A field of 1.3×10^7 V/m applied to Sm is just sufficient to overcome the space charge effects produced by a charge of 170 pC emitted from an illuminated area of about 0.05 mm^2. This corresponds to a current density of 34 kA/cm^2. However, the yield from Mg, having ~3 times the laser energy on a similar area,

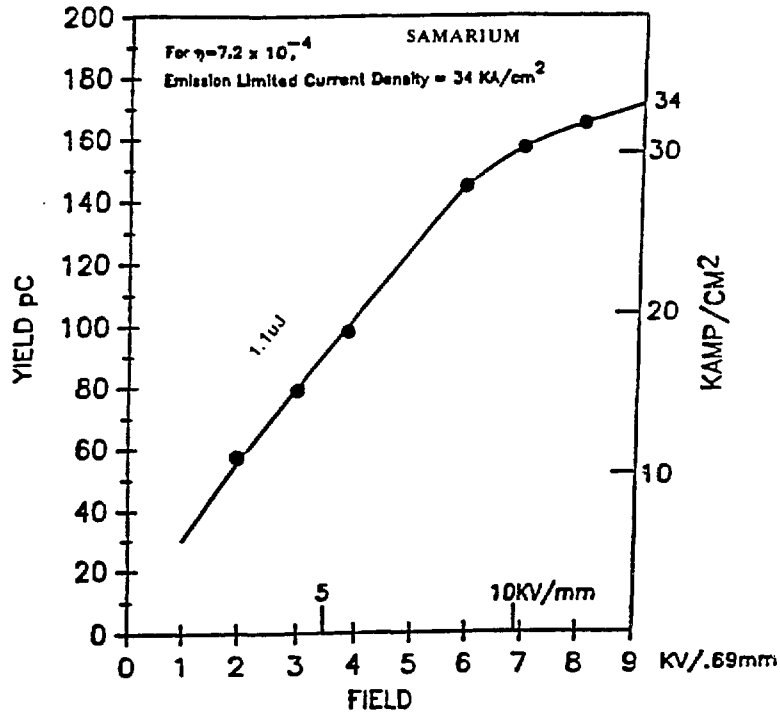

Fig. 4a Charge and current density for samarium, plotted as a function of the applied field. At fields of 10 kV/mm, emission limited operation is barely beginning. Maximum current density obtained for 1.1 μJ energy at 266 nm on a 0.25 mm diam spot is ~34 kA/cm^2. The gap was 0.69 mm.

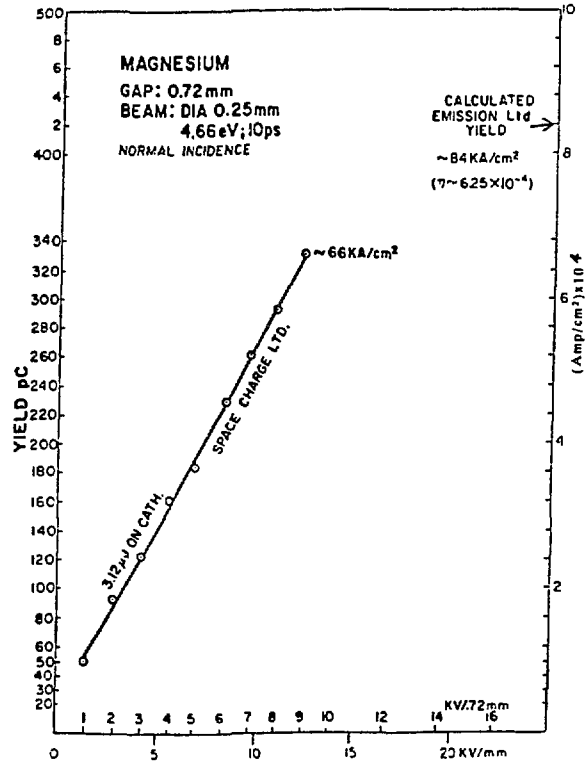

Fig. 4b Charge vs field plot for Mg. The scale on the right is the corresponding current density in a space charge free regime (where electron pulse duration equals laser pulse duration). Even at the maximum field applied, the emission here is space charge limited. If it was space charge free, the expected current density, for a laser energy of 3.1 μJ at 266 nm on a 0.25 mm diam spot and an efficiency of 6.25×10^{-4}, would be ~84 kA/cm^2.

continues to rise linearly with the field, indicating that the space charge is limiting the electron emission even at a field of 1.2×10^7 V/m. The maximum charge and the corresponding current density measured in this space charge limited condition, from the illuminated area of 0.05 mm^2, are 330 pC and 66 kA/cm^2, respectively. Based on the quantum efficiency of 6.25×10^{-4},

listed in Table 1, the emission limited current density for this laser intensity would be 84 kA/cm^2.

A high current photoemission from a larger illuminated circular area of ~7 mm^2, on an heavily activated yttrium cathode is shown in Fig. 5. The charge output is plotted versus the laser pulse energy for applied fields up to 1.6×10^7 V/m.

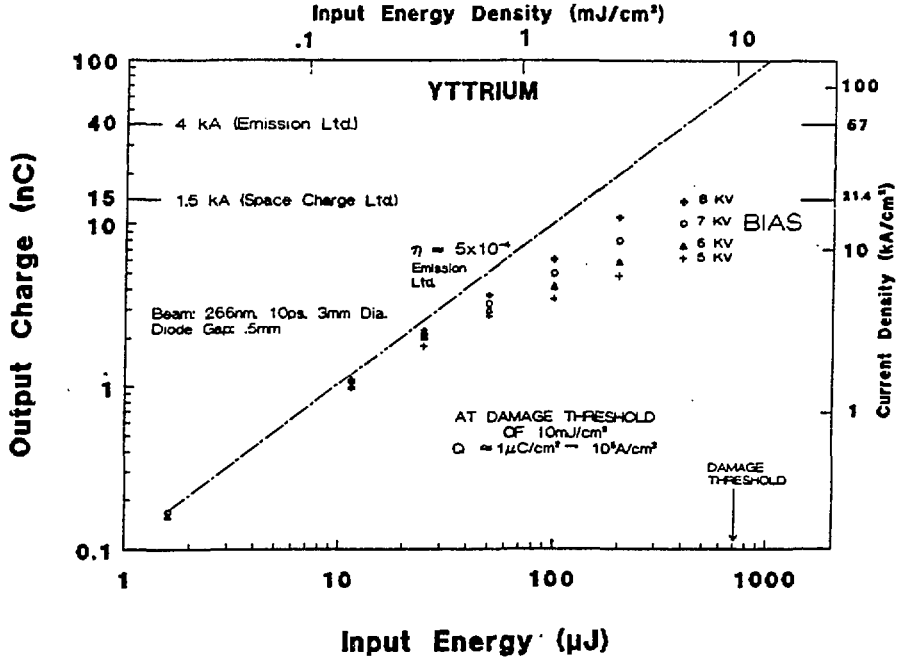

Fig. 5. The electron yield from yttrium as a function of the laser energy for different extraction voltages. Even at an applied field of 16 kV/mm, the maximum emission (15 nC) is limited by the space charge. The emitting area is 7 mm^2 and the corresponding current density is 21 kA/cm^2. It would be ~57 kA/cm^2 without space charge at higher voltages.

For low input energies, the extraction field is large enough to overcome the space charge, and the output charge increases linearly with

the laser energy. But for larger laser energies, the output saturates, indicating the onset of space charge effects. The highest charge extracted in this mode of operation is 15 nC. The corresponding current and current density are 1.5 kA and 21 kA/cm^2, which are the highest current and current density (for 10 ps) reported to date for a macroscopic photoemitter. The emission limited output for the same input of ~400 μJ, but at an adequate field, would be ~40 nC, corresponding to ~4 kA or 57 kA/cm^2. As can be seen from Figs. 4 and 5, the current and the current densities are limited primarily by the extraction field and space charge. The maximum applied dc field in these measurements is 1.6×10^7 V/m, restricted by the electrical breakdown. A pulsed high voltage source that can be synchronized to the laser is currently under construction and is expected to increase the hold off voltage and reduce the space charge effects.

4. CHARGE SPREADING AND MAXIMUM EMITTED CHARGE

In our photodiodes the electron transit time is longer than the laser pulse duration. In the emission limited case without significant space charge, the extracted charge, its duration, and area, would be nearly the same on the anode as on the illuminated cathode. The current would be the charge divided by the laser pulse length.

In the space charge limited condition on larger areas, the emitted charge is limited to a value which reduces the field on the emitting area to

zero. Additional emission would remain on or near the cathode surface. The electron bunch length will increase because the back end of the electron bunch drifts in a lower field than the front end. The space charge limited charge and the current density, and duration on the anode, have been analyzed by Girardeau-Montaut[2] for larger areas. The maximum possible extracted charge is assumed to be equal to the electrostatic charge of the field on the illuminated cathode area.

However, in our experiments we measure emitted charges from the cathode which are much larger than the static charge on the illuminated area. The subsequent section attempts a possible explanation for this phenomenon due to charge spreading. This can be caused by the electrons from the illuminated cathode areas experiencing space charge forces, and the photoelectric process. The charge spreading due to the photoelectric process is due to the isotropic distribution of the velocity of the electrons as they emerge from the surface and is independent of the irradiated spot size. The former effect is due to the Coulomb repulsion experienced by the electrons at the boundary of the bunch and is predominant for narrow dimensions. Figure 6 illustrates the concept.

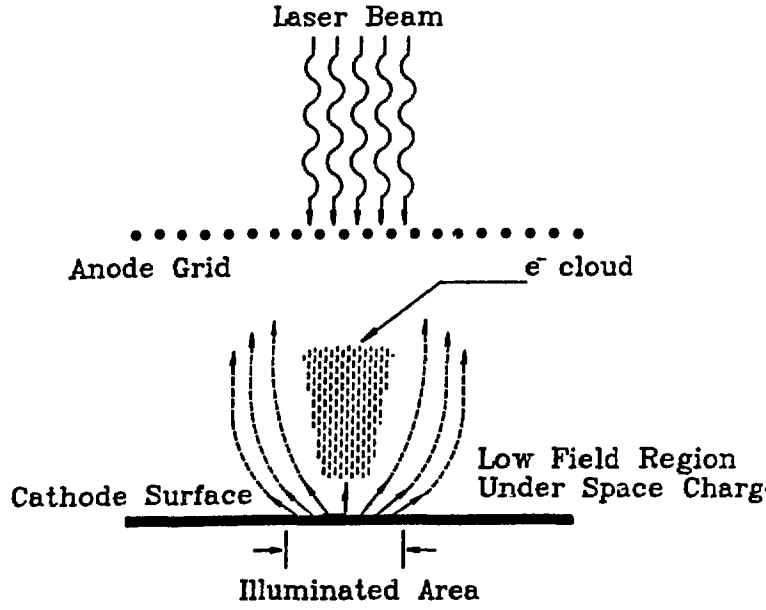

Fig. 6. Charge spreading factors in small diam beams at space charge conditions:
1. Coulomb forces in e^- cloud.
2. Field distortions by space charge.
3. Kinetic energy ($h\nu - \phi$) and direction of photoelectrons in low field volume under space charge.

These effects will be less significant in large diam beams and at much higher fields.

Below the center of the electron cloud, where the field is low, the emission is reduced. Some electrons are driven transversely by the space charge forces to the charge free regions. A stronger effect is due to the kinetic energy of the photoelectrons, i.e., the difference between the photon energy and the work function (about 1.7 eV for yttrium and 4.66 eV photons), and the assumption of a nearly isotropic emission. These electrons have a velocity with a transverse component and will drift sideways until they encounter electric field lines to the anode, around the central space charge cloud.

These two effects result in a larger virtual cathode area than the illuminated area and thus increases the total effective stored and extracted charge from the illuminated cathode area.

Emitted Charge Limits and Illuminated vs Effective Areas

A detailed analysis will not be attempted here but we can compare the calculated static charge using the illuminated area, and the effective area derived from the respective experimental measurements.

The maximum available stored charge Q in a planar diode of gap g, and area A in a field $E = V/g$ is given by Gauss Law

$$Q = \epsilon_0 AE = CV \tag{2}$$

and the capacitance C of a diode is $C = \epsilon_0 \frac{A}{g}$ (3)

and ϵ_0 is the dielectric constant of free space. The above gives us the capacitance C_1 for a diode of a known illuminated area A_1 and gap length g_1. The effective capacitance C_2 in the experiments, is given by the slope $\Delta Q/\Delta V$ of the respective charge vs voltage curves, measured in the space charge limited linear region. Eq. (3) then gives the effective area A_2. The ratio of the observed charge to that of the static charge will be the same as the ratio of the areas.

$$\frac{Q_2}{Q_1} = \frac{C_2}{C_1} = \frac{A_2}{A_1} \tag{4}$$

The subscript 2 denotes the effective values. In the experiments of Fig. 4a and 4b, the gap is about 0.7 mm and the slopes $\Delta Q/\Delta V$ are about 23 fF at

1.1 μJ and about 45 fF at 3.12 μJ. The photon beam had a nominal FWHM diam of 0.25 mm. (The actual area may be twice as large because of diffraction effects, but the illumination energy remained the same.) The resulting charge or area ratios are shown in Table 3.

Table 3

	Sm	Mg
Illumination Energy	1.1 μJ	3.12 μJ
Illuminated Area (cm^2)	5 (to 10) $\times$ 10^{-4}	5 (to 10) $\times$ 10^{-4}
Effective Area (cm^2)	~1.8 $\times$ 10^{-2}	~3.7 $\times$ 10^{-2}
Ratio $\frac{Q_2}{Q_1} = \frac{A_2}{A_1}$	~36 (to 18)	~74 (to 37)

The experimental observations (Figs. 4 and 5) seem to support the model in Fig. 6 at least qualitatively. For small illuminated areas or areas with one small dimension, the effective areas can be substantially larger than the illuminated area. This causes a corresponding increase in the emitted charge and charge density on the emitting area. Furthermore the effective area above the cathode increases with the laser pulse energy. The effects are reduced at higher fields and in large area cathodes.

5. IMPROVEMENTS OF THE QUANTUM EFFICIENCY

Two methods will be described here to increase the efficiency using field assistance with A) Coaxial geometry and B) structured surface. Other methods to increase the efficiency such as multiphotons, polarized beams at grazing incidence and plasmon excitation effects, are described in other papers at this Workshop.

A. Field Assisted Photoemission

As described earlier, the quantum efficiency of the photoemission process can be expressed by Eq. 1, where ϕ is now the effective work function. This work function can be lowered by increasing the energy of the electrons either thermally, electrically, or a combination of both. Increasing the surface field will lower the work function by lowering the effective potential barrier. Fields above 10^9 V/m will also narrow the potential barrier, so that some photoexcited electrons could tunnel through the barrier (photon stimulated field emission). In this region the efficiency can rise very rapidly with the field. Our experiments are below this region, but one may get close to such surface fields because of local enhancement of the applied field due to the microridges normally found in rough surfaces. For fields less than 10^9 V/m, based on the Schottky effect,[9] the lowered effective work function ϕ can be expressed as a function of the zero field work function ϕ_0 and the surface field E. E is the applied field modified by the field enhancement factor β.

$$\phi = \phi_0 - \left(\frac{eE}{4\pi\epsilon_0}\right)^{1/2} \tag{5}$$

By combining the efficiency Eq. (1) with Eq. (5) the field assisted efficiency can be expressed as

$$\eta^{1/2} = A^{1/2}\left(h\nu - \phi_0 + \left(\frac{eE}{4\pi\epsilon_0}\right)^{1/2}\right) \tag{6}$$

where e is the charge of the electron, ϵ_0 is the dielectric constant of free space, A is a material dependent factor and $h\nu$ is the photon energy.

We explored the field assisted efficiency in the Schottky regime for a 4 μm diam gold-coated tungsten wire held coaxially in a cylindrical anode of 1 mm radius.[3] The illuminated wire length was 0.5 mm. This geometry enhances the surface field over the applied field by a factor $\beta \sim 800$, so that surface fields up to 3×10^8 V/m could be explored with moderate dc voltages.

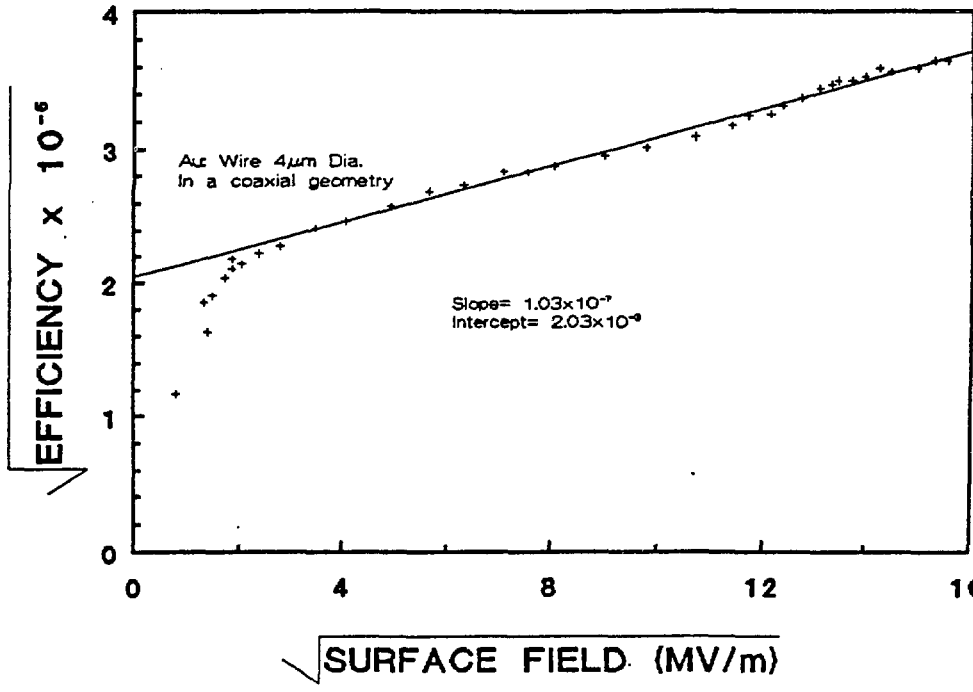

Fig. 7. The root of the efficiency vs root of the surface field for fields up to 2.5×10^8 V/m. The 4 μm diam wire is held coaxially in a cylindrical anode. Laser energy on the wire is .2 μJ. The three to four fold rise in the efficiency is due to the lowering of the work function by the field.

The variation of the field assisted efficiency η with the surface field E for this case, is plotted in Fig. 7 as $\eta^{1/2}$ vs $E^{1/2}$. The straight line part of the curve fits Eq. (6). The efficiency increases by a factor of ~3.5 at $\sim 2.5\times10^{8}$ V/m over the zero field efficiency, which can be obtained from the intercept with the vertical axis. By fitting a line through the data and using ϕ_0, β, and A as variables in Eq. (6), one can obtain approximate values for these quantities. Field assisted efficiency increase was also observed on flat cathodes, but was limited by the permissible dc voltage range. However the surface field and efficiency can be increased also for larger areas as follows.

B. Efficiency Increase by Structured Surfaces and Field Assistance

It is possible to generate a structured surface on a suitable cathode like yttrium by repeated scanning of the surface with intense focused UV laser pulses,[10] so that the surface is modified to result in grainy structure. The grain sizes can be controlled by the beam pulse energy. Figure 8 shows SEM pictures of yttrium structures generated by various scan energies. The quantum efficiency of such surfaces is increased by a combination of effects. The treatment tends to bring to the surface absorbed gases and imbedded impurities, and remove them, so that the work function is lowered to that of a pure metal. Another benefit is the increased light absorption on such rough surface. The efficiency benefits from the enhanced fields on the grainy surfaces. The highest average efficiencies over larger areas are related to the size and the number of grains per unit area, as shown in

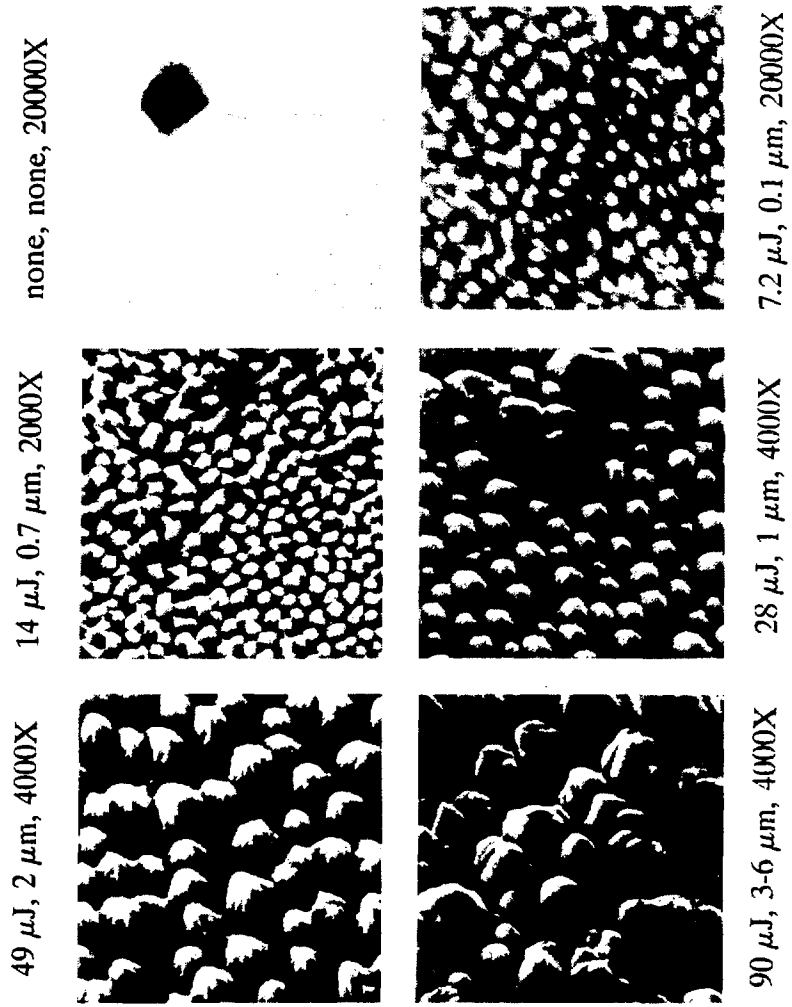

Fig. 8. SEM pictures of six sites on an yttrium surface. Five sites are scanned with UV laser beams of five different energies and one site is unscanned. The scanning energy, grain size and the magnification are marked alongside of each picture. Parameters of the scanning laser: wavelength = 266 nm, pulse duration = 10 ps, spot size = 300 μm FWHM. Each scanned site receives an average of $\sim 6.8 \times 10^4$ pulses/mm^2.

Fig. 9, where the optimum scanning energy is indicated by the curve for the highest average efficiency. The efficiency increased by about a factor of 3 to about 1.3×10^{-3} at an applied field of 1.3×10^{7} V/m. The average field enhancement factor for the top curve is about 7–8 using Eq. (6). The peak field enhancement factor on top of the grains is probably higher. It is possible that at higher (pulsed) fields on such surfaces, one may reach the region of photon stimulated field emission and much higher efficiencies.

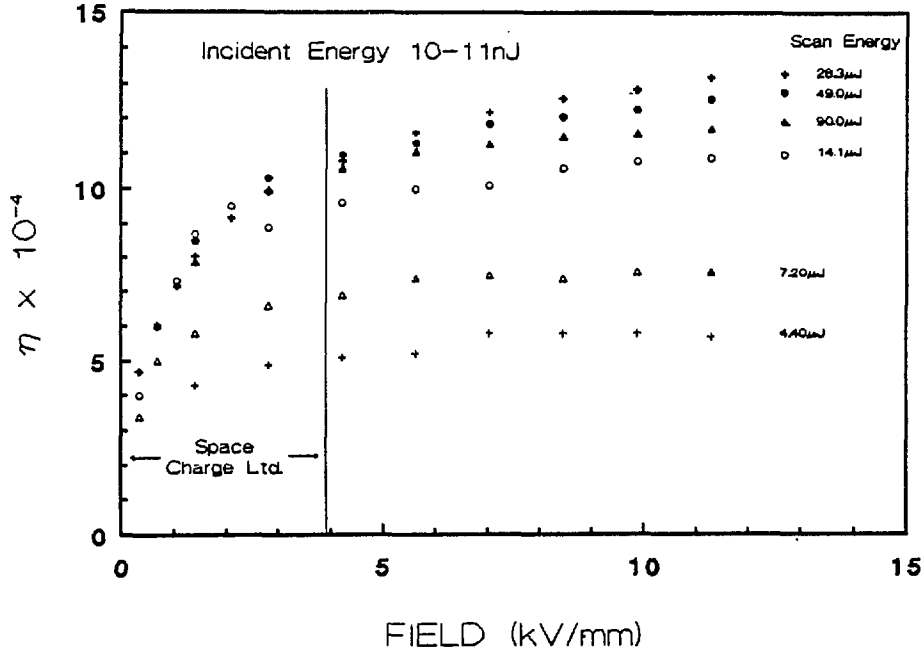

Fig. 9. Dependence of the efficiency on the applied field, for different scanning energies. For fields >4 kV/mm the efficiency at any given field is given by the corresponding y-coordinate.

This is illustrated in Fig. 10 with an extension of the line through the data taken for the y surface scanned with 28.3 μJ laser beam. However even considering the Schottky effect alone, efficiencies of over .25% are likely at applied pulsed fields of 10^8 V/m. It is not yet known if structured yttrium can withstand such fields without breakdown.

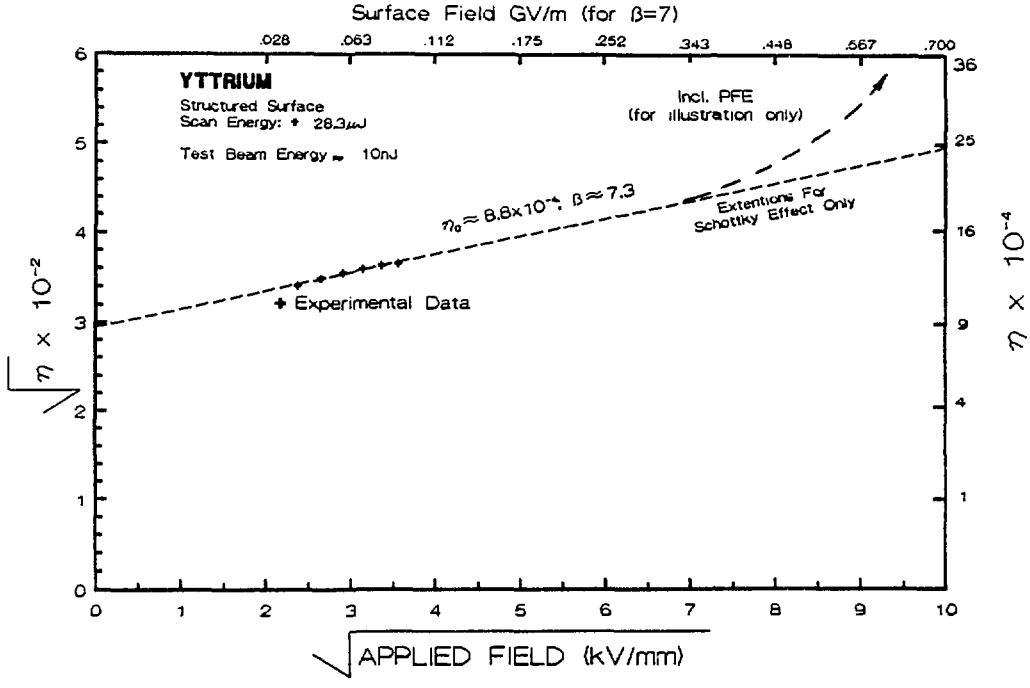

Fig. 10. The root of efficiency vs the root of the field using the data points for the yttrium surface scanned by 28.3 μJ (Fig. 9). The line is extrapolated to applied fields of 10^8 V/m for a β of 7. The extended line illustrates the expected large increase in efficiency and the onset of tunnelling at very high fields.

6. HIGH VOLTAGE BREAKDOWN CONSIDERATIONS

In many applications very high fields are required for high current densities, high efficiency and to avoid space charge effects. Therefore, the holdoff fields of cathodes have to be explored.

A. RF Guns with Photocathodes

In collaboration with the staff of the Accelerator Test Facility at BNL, we have investigated a flat yttrium photocathode of 6 mm diam, embedded in a copper holder in an RF gun.[11] The gun operated near 3 GHz with ~2 μs bursts, at 3 to 10 Hz, and produced cathode surface fields near 100 MV/m without breakdown. The cathode was illuminated with an excimer KrF laser providing 20 ns pulses at 248 nm.

Maximum RF breakdown surface fields for copper in resonant wave structures at SLAC were reported by Loew and Wang[12] for ~2 μs bursts of RF at 2.9, 5, and 93 GHz. After considerable "training," they obtained breakdown fields of about ~300, 420, and 600 MV/m, respectively. For safe operation one would probably use lower fields. The breakdown field as a function of frequency seems to behave as

$$E_s \sim 195\,[f(\mathrm{GHz})]^{1/2} \quad \mathrm{MV/m} \tag{7}$$

B. DC and Pulsed High Voltage Photodiodes

Experience with flat y photodiodes in our test cell, dc HV, indicates breakdown at fields of 25 MV/m with 0.3 mm gaps.

In order to simulate conditions at the SPL or in similar applications, pulsed fields are required. These have much higher breakdown values for short pulses. An example is shown in Fig. 11 for a graph of the breakdown field vs time to breakdown, after Evans et al.,[13] for aluminum electrodes and small gaps for pulse times below 0.5 ns. Values for 1, 5, and 10 ns, are

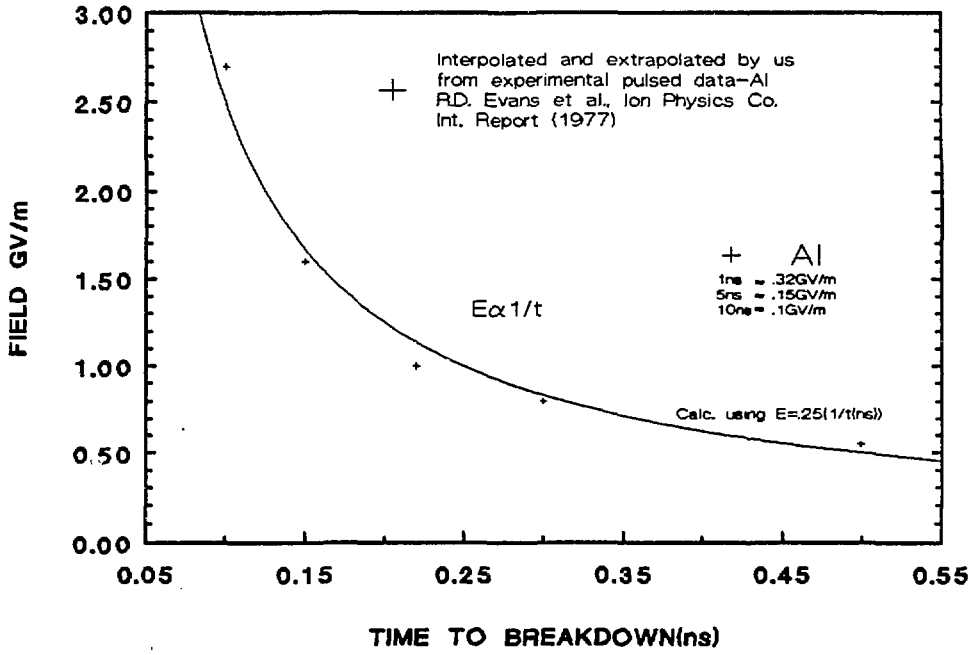

Fig. 11. Breakdown fields up to 3 GV/m vs the time to breakdown below 1 ns for aluminum electrodes.

also indicated. Fields of several GV/m seem possible, e.g., 1 GV/m at 0.3 ns. For aluminum the relationship is approximately:

$$E_S \sim .25\left(\frac{1}{t_{(ns)}}\right) \text{ GV/m} \tag{8}$$

The breakdown fields vary with the type of metal. In Fig. 12 are graphs of breakdown fields and time to breakdown given for Mo ≈ (W), Cu, Al, Pb and C in the 1 to 20 ns range (adapted from Mesyat, et al.[14]), Mo having the highest value. It seems that hard metals, or alloys of high melting temperatures, can withstand higher fields.

We are considering such metals in pulsed photodiodes with and without structured surfaces as alternatives to yttrium or copper because they may be more durable and stand higher fields. Their higher work function can be tolerated, since the efficiency is expected to be strongly assisted by surface fields, near photofield emission.

For safe operation the HV pulse duration will have to be shorter than indicated in the graphs. Pulses in the 10 ps range and GV/m fields, will be encountered at the photocathode e^- beam source in the center of the first SPL section (Fig. 1). On the other hand the ring cathode will have to hold off the highest fields possible for 1–2 ns.

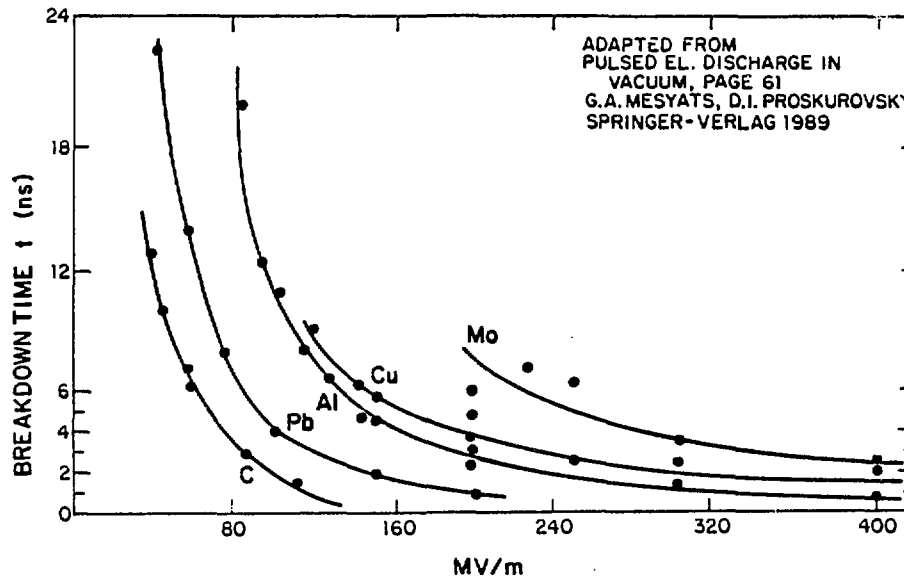

Fig. 12. Breakdown time vs the field in the 1–20 ns region for various metals.

CONCLUSIONS

Based on our measurements of quantum efficiencies and damage thresholds with 10 ps, 266 nm UV pulses, it seems feasible to obtain current densities exceeding 100 kA/cm^2 from macroscopic areas, limited by space charge and available extraction fields. Yttrium or copper seem practical for high current applications.

A significant charge spreading effect above the cathode surface was observed with narrow illuminated areas, in the space charge limited regime. Such effects would spoil the quality of high brightness electron beams. At the SPL which has a narrow ring-shaped cathode, charge spreading increases the width and transit time of the charge. This would increase the rise time and duration of resulting E&M pulse and reduce the field at the center of the SPL discs. Experimental evidence indicates that the emittance of the electrons decreases considerably when *p*-polarized laser beam incidents on the surface at grazing incidence. This effect may also be used to reduce electron spreading. (Emission angles near 10° are reported by Toth and Farkas, et al., at this Workshop.)

Field assisted increases of efficiencies by a factor of 3 resulting in an efficiency of 1.4×10^{-3} were obtained at moderate dc fields from a micro-structured yttrium surface, having a field enhancement factor of 7–8. A much higher efficiency can be expected in the SPL with applied pulsed fields of several 10^8 V/m if there is no breakdown. It remains to be explored if

microstructured cathodes of Mo, W, or Ta, which are known to sustain higher fields, will result in safe operation and high efficiencies at pulsed surface fields around 10^9 V/m.

ACKNOWLEDGEMENTS20

The authors would like to thank Drs. V. Radeka, W. Willis and R. B. Palmer for their insightful discussions and support. They also would like to thank N. Schaknowski, M. Stuff and John Schill for their expert technical assistance.

REFERENCES

1. W. Willis, in *Proceedings of the Second Conference on Laser Acceleration of Particles*, edited by C. Joshi and T. Katsouleas, AIP conference Proceedings, Vol. 130 (American Institute of Physics, New York, 1985), p. 242.

2. J. Girardeau-Montaut and C. Girardeau-Montaut, J. Appl. Phys. **65**, 2889 (1989).

3. J. Fischer, T. Srinivasan-Rao, in *Proceedings of New Developments in Particle Acceleration Techniques*, Orsay, 1987, ed., S. Turner, CERN 87-11 ECFA 87/110, p. 506.

4. J. Fischer, T. Srinivasan-Rao, T. Tsang, in *Proceedings of the Switched Power Workshop*, Shelter Island, New York, 1988, ed., R. Fernow, BNL 52211, p. 44.

5. R. C. Weast, ed., *CRC Handbook of Chemistry and Physics*, (CRC Press, Boca Raton, FL, 1979).

6. M. Cardona and L. Ley, in *Photoemission in Solids*, ed., M. Cardona and L. Ley (Springer-Verlag, New York, 1978), p. 23.

7. P. May, J.-M. Halbout, and G. Chiu in *Picosecond Electronics and Optoelectronics II*, ed., F. J. Leonberger, C. H. Lee, F. Capasso, H. Morkoc (Springer-Verlag, New York, 1987), p. 54.

8. P. B. Corkum, F. Brunel, N. K. Sherman and T. Srinivasan-Rao, Phys. Rev. Lett. **61**, 2886 (1988).

9. W. Schottky, Z. Phys. (in German) **14**, 63 (1923).

10. T. Srinivasan-Rao, J. Fischer, T. Tsang, to be published in J. Opt. Soc. Am. B.

11. K. Batchelor, et al., "Operational Status of BNL Accelerator Test Facility," to be published in the Proc. of the 1990 European Accelerator Conf., Nice, France, June 12-16, (1990).

12. J. W. Wang and G. A. Loew, SLAC 4866 (1989).

13. R. D. Evans, et al., Ion Physics Co., USA, Internal Report (1977).

14. Adapted from G. A. Mesyats and D. I. Proskurovsky, *Pulsed Electric Discharge in Vacuum*, New York, Springer-Verlag, (1989), p. 61.